SYNTHESIS, CHARACTERIZATION AND PROCESSING OF NEW MATERIALS FOR INNOVATIVE APPLICATIONS
Jan-Jun 2025, VOL. 2, ISSUE 1, pp. 28-37
https://doi.org/10.61577/scpnmia.2025.100003

RESEAPRO JOURNALS

ORIGINAL ARTICLE

OPEN ACCESS

A study on approaches to uncertainty assessment in XRD analysis for determining inorganic compounds in complex waste materials

Daniela Rizzo[1], Debora Cusumano[1], Laura Borgese[2], Annalisa Zacco[2], Eleonora Cuccia[3], Silvia Maltese[4] and Marco Volante[4]

[1]U.O. Laboratorio Regionale Area Est – Dipartimento Prestazioni Analitiche – ARPA Lombardia, Via Cantore 20, 25128 Brescia, Italy
[2]Dipartimento di Ingegneria Meccanica ed Industriale, DIMI - Università di Brescia - Via Branze 38, 25123 Brescia, Italy
[3]U.O. Qualità dell'Aria - Direzione Generale – ARPA Lombardia, Via Rosellini 17, 20124 Milano, Italy
[4]U.O. Accreditamento e Sviluppo Tecnico Scientifico - Dipartimento Prestazioni Analitiche – ARPA Lombardia, Via Rosellini 17, 20124 Milano, Italy

ABSTRACT

A study was done to estimate the uncertainty of waste analysis by XRD technique on powder samples. The XRD technique is important for identifying crystalline phases and inorganic compounds to give information about hazardousness on unknown wastes. No reference materials or proficiency tests are available for these sometimes very complex and heterogeneous matrices. The present study was done on a real sample with a metrological approach. The matrix complexity in the considered sample, even after grinding, is increased by the fact that there is a fibrous fraction and a nonfibrous powdery fraction mixed together. Accuracy was checked by analysis with other techniques and at other laboratories. The results showed that external calibration with single pure standard is prone to large errors compared with the use of multi-level external calibration. The approach that best accounts for matrix complexities is however the method of standard additions. The level of uncertainty determined was within ±50% as the expanded uncertainty (k≈2, conf. level 95%).

KEYWORDS

Wastes; X-Ray diffraction; Uncertainty

ARTICLE HISTORY

Received 19 December 2024; Revised 20 January 2025; Accepted 27 January 2025

Introduction

Waste is an extremely complex matrix from the point of view of the analytical characterization. The term "waste" can include all types of materials, organic, inorganic or mixed in a solid, liquid or even muddy state [1]. Environmental protection agencies tasked with monitoring unknown or suspicious waste frequently need to assess their hazardousness [2-4]. To achieve this, chemical analysis and detailed characterization are routinely employed.

Chemical analysis capable of identifying a wide range of organic and inorganic contaminants, often provides information only on a limited part of the sample. For this reason, a laboratory may also be asked for further information on the sample's matrix and its hazardousness. To answer these questions, our laboratory -upon request- has activated routine screenings of inorganic and organic substances on waste samples using complementary techniques like the X-Ray Powder Diffraction (or also XRPD) side by side with Gas Chromatography-Mass Spectrometry (GC-MS). The technical standards referred to are EN 13925 (XRD) and EPA 8270, EPA 8260 (GC-MS) [5-7].

In the case of organic and inorganic substances investigated on the matrix of an unknown waste, various compounds or crystalline phases included among almost all existing organic and inorganic substances can potentially be found. This involves maintaining in operation an extremely large pool of calibration standards substances to be managed and ensured to be efficient within the expiry dates of the materials. On the other hand, the application of a large but limited panel of routinely analyzed substances (as for metal analyses using ICP or volatile organic substances determined via GC/MS) may result as not effective. EPA technical standards 8260 and 8270 provide some guidance for the identification and quantitation of "untargeted analytes" in paragraphs 11.6 and 11.7. The EN 13925 standard contains limited indications [8], in this case, for the quantitation of the crystalline phases.

Furthermore, in the case of waste, the uncertainty linked to analytical determination can strongly depend on the complexity of the matrix, on the interferences originating from it and on its difficulty in being homogenized in the preparatory phases.

This work describes a case of identification by X-Ray Powder Diffraction of Rutile in the crystalline phase, probably in the form of a finely divided industrial powder retained in exhausted filters made of plastic mixed with vitreous fibers. In this approach, working on a very complex matrix, uncertainty is estimated in a precautionary form. The uncertainty is estimated both in the case where the quantification of the found phase is quickly carried out by direct comparison with 100% pure substance and in the case in which it is carried out more accurately with the standard addition method. The study also aims to highlight the challenges associated with assessing measurement uncertainty in waste matrices.

***Correspondence:** Dr. Daniela Rizzo, Department of Analytical Services, Regional Laboratory Unit, Regional Environmental Protection Agency of Lombardy, Cantore Street, Brescia, Italy. e-mail: D.RIZZO@arpalombardia.it

RESEAPRO JOURNALS

Material and Methods

A sample of exhausted filters was obtained from control programs performed from Laboratory A (ARPA Lombardia/East Area Laboratory/Brescia) and anonymized for the purpose of this study. The sample was dried at 40°C and initially crushed into particles smaller than 4 mm, using a Fritsch Pulverisette 1 jaw crusher and successively ground in a Retsch ZM200 centrifugal mill to particles size less than 1 mm. The ground sample was finally sieved in a 0,5 mm sieve.

Instrumental analyses were carried out on a Siemens Kristalloflex D5000 X-Ray diffractometer with a radiation source Cu K-α (λ = 0,15406 nm) and working with 40 kV voltage and 30 mA current intensity. The XRD diffractograms were recorded on a 2 g sample portion, from 2θ = 5° to 2θ = 55° with 2θ increments of 0,02° per second. Mineral & Master libraries databases. EVA 2 SocaFile library, version 3.00.57 (2002) and AboutBox library, version 1.06.86 (2000).

Both pure standards, TiO2 (Rutile, CAS 1317-80-2), cod. 224227-100G, lot MKCD8026 99,9% and TiO2 (Anatase, CAS 1317-70-0), cod. 232033-100G, lot MKCD6078 - 99,8% were purchased from Sigma Aldrich. The XRD analysis of pure Rutile revealed the presence of additional peaks corresponding to Anatase impurities. The Anatase impurities resulted to be 4,9% with quantitation by standard addition performed by Laboratory A. Laboratory C (University of Brescia/DIMI) established a true Rutile content of 95% and an Anatase content of 5% based on XRD analysis with Rietveld and RIR methods. Pure Rutile standard at 100% nominal concentration was thus considered in all calculations of this study as 95% pure.

Laboratory materials for multi-level calibration were done by Laboratory A by mixing and grinding in an agata mortar pure Rutile at different weight percentages (10%, 20%, 40%, 50%, 75%) with Extrelut. Extrelut siliceous earth (free from silicic acid crystals) or also diatomaceous earth (CAS 68855-54-9) was purchased from Sigma Aldrich. Laboratory materials for multi-level calibration were also given to Laboratory B (ARPA Lombardia/Air Quality Unit/Milan) and to Laboratory C for calibrations.

XRF measurements and quantitation for accuracy verification were conducted by Laboratory B using a Panalytical Epsilon 4 XRF spectrometer. The sample was analysed by placing the powder inside a sample holder consisting of a support ring and a Mylar membrane. This membrane has no relevant absorption of X-ray radiation and can be considered irrelevant for XRF analysis. The powder was placed in the sample holder to create a layer as thin as possible.

XRD measurements and quantitation for accuracy verification were performed by Laboratory C using a Panalytical X'Pert PRO XRD diffractometer equipped with a X'Celerator detector. The X-ray source was Cu Kα (λ = 0.154nm) with generator settings of 40 mA, and 40 kV. XRD patterns were collected at room temperature over 2θ range of 10° ÷ 100° 2θ (Step Size: 0.017° 2θ; Scan Step Time: 18 s). Spectral analysis was carried out using X'Pert Highscore Plus software.

Results and Discussion

Figure 1-a presents the material used in this study. The image depicts the exhausted filter sample prepared for the leaching test, following the EN 12457-2 standard, by crushing it to a particle size of less than 4 mm. The notable heterogeneity of the sample is clearly visible in the image. Figure 1-b shows the ground sample using a ZM-200 Retsch centrifugal mill; in this case the particle sizes were further reduced to less than 1 mm and as a result the material appears s a poorly homogenized set of fibrous and non-fibrous particles.

Figure 1. 1-a (left): the whole waste sample as crushed <4 mm in the cutting mill for the leaching test, according to standard EN 12457-2; 1-b (right): the whole waste sample as ground <1 mm in the centrifugal mill.

In this phase, grinding to particle sizes smaller than 100 microns becomes impracticable due to sample overheating and the melting of the plastic materials present in the waste. This melting irreversibly clogs the filter pores even at dimensions of 500 microns. Furthermore, the fibrous particles, if present, can pass the filter exhibiting dimensions close to 100 microns in section although even greater than e.g. 500 microns in the length direction.

In order to work on more homogeneous materials, it was decided to separate the dusty and non-fibrous fraction (Fig. 2-b) from the fibrous fraction (Fig. 2-a) by sieving at 500 microns and obtaining two subsamples. The non-fibrous powdery phase, determined by weighing, was found to be equal to 81% by weight. On the other hand, the fibrous fraction was found to be equal to 19% by weight. Repeatability tests were conducted on the two separate fractions by means of replicate analyses of the titanium oxide (rutile) content.

https://doi.org/10.61577/scpnmia.2025.100003

RESEAPRO JOURNALS

Figure 1. 2-a (left): the waste sample as ground <1 mm in the centrifugal mill, fraction passing through a 0,5 mm sieve and predominantly powdery and non-fibrous; 2-b (right): the waste sample as ground <1 mm in the centrifugal mill, oversize fraction through a 0,5 mm sieve and predominantly fibrous.

Figure 3 shows the X diffractogram obtained for the investigated waste, compared with a 95% pure Rutile standard. Table 1 summarizes the Rutile peaks identified through the instrument's spectral library [9], supplemented by a review of relevant literature data [10–11]. The remaining peaks of the standard (main lines 2θ = 25.22°, 37.69° and 47.85°) were identified as Anatase impurities [10] and determined to be 5%. The very enlarged signal in the waste sample was assigned to the presence of amorphous vitreous substance coming from glass fibers of the filtering materials.

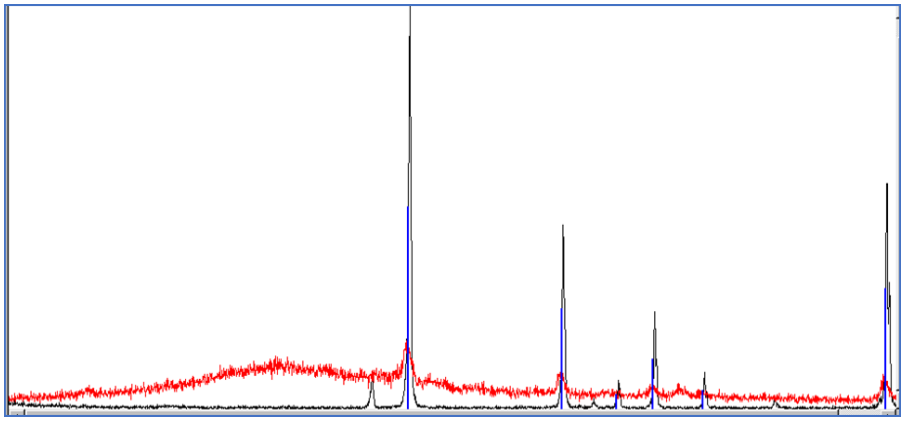

Figure 3. Labaratory A. The XRD powder diffractogram of the entire waste sample (red trace) compared with the pure Rutilus standard (black trace). Diffraction signals of the Rutile standard not marked with blue rods are related to Anatase impurities. Note the baseline bias in the sample, likely indicate the diffraction of the amorphous phase attributed to vitreous fibres. The 2Θ scale ranges from 5° to 55°.

Table 1a. Rutile main diffraction data obtained for in the present work compared with 2θ values of the same diffraction lines from literature.

RRUFF ID[10]	**Main diffraction lines considered**						**RRUFF source description**
	1	**2**	**3**	**4**	**5**	**6**	
Rutile R060745	27.40°	36.03°	39.06°	41.20°	43.95°	54.25°	Herb Obodda 091; Zagi Mountain near Hammedabad, Knaffor Dehri, NW Frontier Provence, Pakistan
Rutile R110109	27.38°	35.98°	39.09°	41.12°	43.93°	54.17°	Gemological Institute of America 10-12-2010-14; Synthetic
Rutile R120008	27.11°	35.57°	38.71°	40.66°	43.50°	53.57°	Rob Lavinsky; Golconda, Minas Gerais, Brazil
Rutile R060493	27.50°	36.14°	39,24°	41.30°	44.09°	54.37°	Michael Scott S100359; Diamantina, Minas Gerais, Brazil
Rutile R050417	27.50°	36.15°	39.26°	41.32°	44.11°	54.35°	Marcus Origlieri; Champion mine, Mono County, California, USA
Rutile R050031	27.47°	36.12°	39.23°	41.29°	44.08°	54.37°	University of Arizona Mineral Museum 3776; Chester City, Pennsylvania, USA
Rutile R040049	27.50°	36.13°	39.23°	41.29°	44.09°	54.37°	University of Arizona Mineral Museum 8286; Graves Mountain, Lincoln County, Georgia, USA
ARPA Lombardia (Lab A)	**Main diffraction lines observed**						**Description / References**
Present paper	27.46°	36.01°	39.19°	41.29°	44.0°	54.36°	Investigated waste sample / Rutile Standard
S. Marmai et al.	27.49°	36.15°	39.22°	41.27°	44.09°	54.38°	[11]

https://doi.org/10.61577/scpnmia.2025.100003

Table 1b. Anatase main diffraction data obtained for in the present work compared with 2Θ values of the same diffraction lines from literature.

RRUFF ID [10]	**Main diffraction lines considered**			**RRUFF source description**
	1	**2**	**3**	
Anatase R060277	25.23°	37.72°	47.89°	Herb Obodda 064 Taftan, near Dalbandi, Baluchistan Province, Pakistan
Anatase R070582	25.28°	37.68°	48.01°	Asker, Akershus, Norway
Anatase R120013	25.07°	37.67°	47.53°	Governor's Lake pegmatite, Halifax County, Nova Scotia, Canada
Anatase R120064	25.36°	37.87°	48.16°	East Kemptville Tin mine, East Kemptville, Argyle, Yarmouth Co., Nova Scotia, Canada
ARPA Lombardia (Lab A)	**Main diffraction lines observed**			**Description**
Present paper	25.22°	37.69°	47.85°	Rutile Standard (Anatase impurities) / Anatase Standard

In Figure 4 the complete XRD diffractogram recorded from Laboratory C on the predominantly dusty fraction of the sample, from 2Θ = 10° to 2Θ = 100°, is shown. The main and useful diffraction lines fall in the 2 Θ = 10°-55° range. The other signals are of minor importance for the analysis, due to their low intensities.

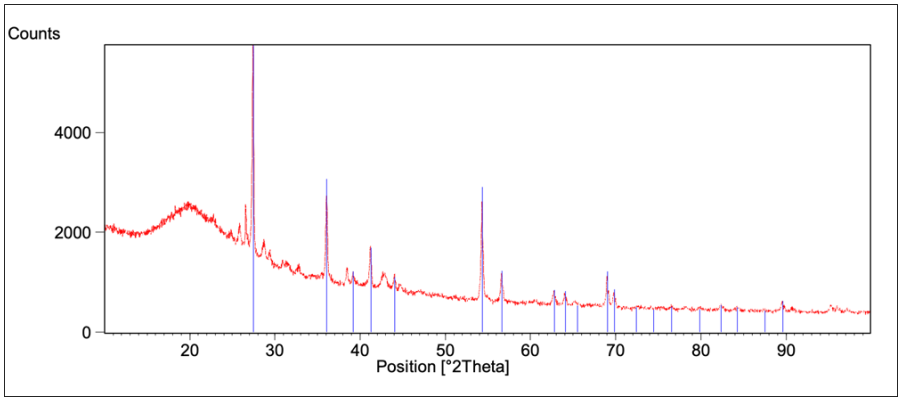

Figure 4. Laboratory C. Complete XRD powder diffractogram obtained on the non-fibrous fraction of the sample (red trace) showing all the Rutile diffraction lines. 2Θ scale from 10° to 100°.

Laboratory A decided to carry out measurements using the most intense diffraction signals (2 Θ = 27.46°, 36.10°, 41.29° and 54.36°). Laboratory A in many cases has given answers only on the qualitative identification of the crystalline species present (e.g. oxides) as a support for the determinations of the quantified metals with the ICP-OES technique, to tentatively identify the inorganic/crystalline species. In other cases, upon request to proceed with quantitative XRD determinations of crystalline inorganic species, Laboratory A has chosen, in a first approach, calibration with an external standard adopting multiple concentration levels or, alternatively, the direct comparison with pure substance. Laboratory A plans to subsequently develop an approach with the RIR (Relative Intensity Ratio) method [12-14] on these types of matrices, identifying an adequate internal standard.

In Figure 5a and 5b the calibration graphs for the 2Θ = 27.46°, 41.29° and 54.36° signals are shown. The signal at 2Θ = 36.10° is not considered as it is interfered by the peaks of the diatomaceous earth used as a solid diluent for the pure Rutile standard. Laboratory A used the average response factors – Rf27,46° and Rf54,36° measured on the calibration points up to the Rutile concentration level of 47.5% (50% theoretical). For concentrations higher than 50%, a saturation of the signal is observed with a noticeable loss of linearity.

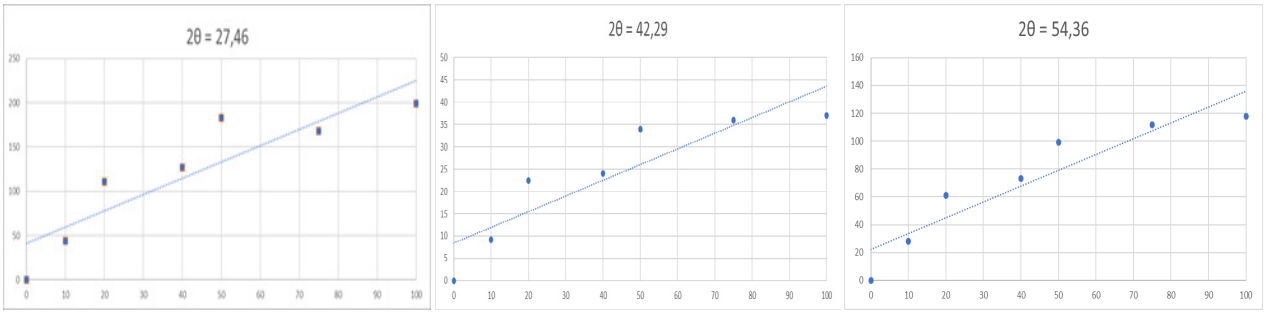

Figure 5a. Laboratory A. XRPD calibration graphs for the signals at 2Θ 27.46°, 41.29° and 54.36°. Signal area (arbitrary units) versus TiO_2 nominal concentration (% units). Range from 10% TiO2 to 100%. Linear function is showed only to highlight the lack of linearity above 50% TiO_2.

https://doi.org/10.61577/scpnmia.2025.100003

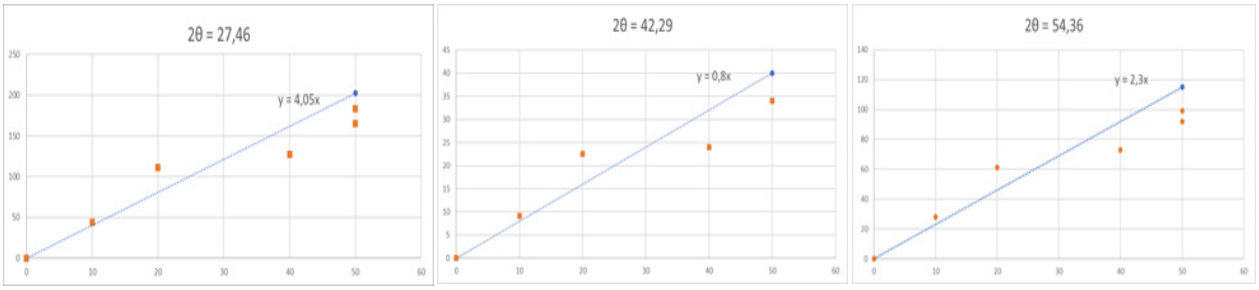

Figure 5b. Laboratory A. XRPD calibration graphs for the signals at 2Θ 27.46°, 41.29° and 54.36°. Signal area (arbitrary units) versus TiO2 nominal concentration (% units). Mean response factor (Rf) calculated for the concentration range 10%-50% TiO2.

Table 2 shows the response factors measured for the three diffraction signals at 2Θ = 27.46°, 41.29° and 54.36° with increasing concentrations, the average value and the absolute and relative standard deviation (CV%). The other diffraction signals (e.g. 2Θ = 39.19° and 44.00°) with response factor variability higher than 30% (as relative standard deviation) were not considered.

Nominal concentration (%)	Rf (2Θ = 27.46°)	Rf (2Θ = 41.29°)	Rf (2Θ = 54.36°)
10% Rutile	4.40	0.92	2.80
20% Rutile	5.55	1.13	3.05
40% Rutile	3.18	0.60	1.83
50% Rutile	3.66	0.68	1.98
50% Rutile	3.30	0.68	1.84
75% Rutile	*2.20*	*0.48*	*1.49*
100% Rutile	*1.99*	*0.37*	*1.18*
Average Rf (0-50% concentr.)	**4.02**	**0.80**	**2.30**
Standard Dev. (0-50% conc.)	**±0.981**	**±0.217**	**±0.581**
Relative CV% (0-50% conc.)	**±0.244**	**±0.271**	**±0.253**

Tables 3a and 3b report six replicate measurements for the non-fibrous dusty fraction, excluding two highly anomalous measurements that were discarded a priori due to high background noise and nearly absent signals. Tables 4-a and 4-b present eight initial replicate measurements for the fibrous fraction, supplemented with an additional six replicates to address the significant variability and weak signals observed in this fraction, resulting in a total of fourteen replicate measurements.

For the two fractions, the average values and repeatability uncertainties are listed (for a single measurement) expressed as absolute and relative standard deviation (CV%) as determined for the three different diffraction signals 2Θ = 27.46°, 41.29° and 54.36° and adopting respectively, for the two calibration approaches, the response factors Rf27,46°, Rf41,29° and Rf54,36° or the signals at 2Θ = 27.46°, 41.29° and 54.36° of the pure 95% Rutile standard (100% theoretical).

Table 3a. Laboratory A. Rutile concentration (weight %) in dust fraction as determined for each diffraction line chosen in the six replicates, using averaged response factor (Rf) calibration.

Replicate→ 2Θ ↓	1	2	3	4	5	6
27,46°	11.50%	10.79%	8.74%	11.02%	8.91%	11.78%
41,29°	13.06%	14.25%	10.95%	15.44%	10.69%	13.67%
54,36°	11.98%	11.56%	9.63%	11.56%	9.50%	12.11%

Table 3b. Laboratory A. Rutile concentration (weight %) in dust fraction as determined for each diffraction line chosen in the six replicates, using pure standard (100% nominal concentration) single point calibration.

Replicate→ 2Θ ↓	1	2	3	4	5	6
27,46°	23.39%	21.96%	17.79%	22.44%	18.14%	23.98%
41,29°	28.24%	30.81%	23.69%	33.38%	23.11%	29.55%
54,36°	23.35%	22.54%	18.78%	22.54%	18.52%	23.61%

Table 4a. Laboratory A. Rutile concentration (weight %) in fibrous fraction as determined for each diffraction line chosen in the fourteen replicates, using averaged response factor (Rf) calibration.

Replicate ® 2Θ ↓	1	2	3	4	5	6	7	8	9	10	11	12	13	14
27,46°	5.26%	5.72%	6.15%	6.24%	6.29%	6.44%	5.99%	5.40%	6.41%	4.74%	6.58%	7.00%	6.96%	5.40%
41,29°	1.54%	2.96%	2.48%	3.13%	4.70%	3.14%	2.21%	3.03%	1.94%	4.28%	0.86%	2.98%	5.83%	3.56%
54,36°	5.38%	2.96%	2.48%	1.53%	2.50%	4.37%	3.71%	2.35%	2.49%	2.59%	4.47%	5.11%	5.80%	3.72%

https://doi.org/10.61577/scpnmia.2025.100003

RESEAPRO JOURNALS

Table 4b. Laboratory A. Rutile concentration (weight %) in fibrous fraction as determined for each diffraction line chosen in the fourteen replicates, using pure standard (100% nominal concentration) single point calibration.

Replicate ® 2θ ↓	1	2	3	4	5	6	7	8	9	10	11	12	13	14
27,46°	10.71%	11.64%	12.50%	12.70%	12.79%	13.10%	12.21%	10.98%	13.05%	9.64%	13.41%	14,25%	14,17%	10,98%
41,29°	3.34%	6.42%	5.36%	6.76%	10.17%	6.77%	4.78%	6.55%	4.19%	9.25%	1.85%	6,44%	12,61%	7,18%
54,36°	10.48%	5.77%	4.83%	2.98%	4.87%	8.53%	7.25%	4.57%	4.85%	5.06%	8.73%	9.96%	11.30%	7.26%

Table 5a. Laboratory A. Mean, standard deviation and CV% as determined for the replicates respectively in the cases of the dust fraction and the fibrous fraction. Calibration has been obtained using averaged response factor (Rf).

Dust, non-fibrous fraction (81% w/w)				Fibrous fraction (19% w/w)			
2θ	Average	Std. Deviation	CV%	2θ	Average	Std. Deviation	CV%
27,46°	10.46%	±1,31%	±12.5	27,46°	6.04%	±0.66%	±11.0
41,29°	13.02%	±1.87%	±14.4	41,29°	3.05%	±1.29%	±42.4
54,36°	11.06%	±1.18%	±10.6	54,36°	3.53%	1.32%	±37.3

Table 5b. Laboratory A. Mean, standard deviation and CV% as determined for the replicates respectively in the cases of the dust fraction and the fibrous fraction. Calibration has been obtained using pure standard (100% nominal concentration) single point.

Dust, non-fibrous fraction (81% w/w)				Fibrous fraction (19% w/w)			
2θ	Average	Std. Deviation	CV%	2θ	Average	Std. Deviation	CV%
27,46°	21.28%	±2.67%	±12.5	27,46°	12.40%	±1.35%	±11.0
41,29°	28.13%	±4.04%	±14.4	41,29°	6.55%	±2.78%	±42.4
54,36°	21.56%	±2.29%	±10.6	54,36°	6.89%	2.57%	±37.3

Tables 5a and 5b list, for the two fractions, the averages, the repeatability uncertainties (considering a single measurement, in analysis) expressed as absolute and relative standard deviation (CV%) and as determined for the three different diffraction signals 2θ = 27.46°, 41.29° and 54.36° adopting respectively, for the two calibration approaches, the response factors Rf27,46°, Rf41,29° and Rf54,36° or the signals at 2θ = 27.46°, 41.29° and 54.36° of the pure standard, 95 % Rutile (100% theoretical).

In Tables 6a and 6b, for the three different diffraction signals 2θ = 27.46°, 41.29° and 54.36° and with the two calibration modes, the following are also listed: a) the average value of all the results obtained on the two, dusty and fibrous fractions, weighed on the percentages (81% and 19% by weight) of the two fractions themselves; b) the repeatability uncertainty estimated as a combination of the uncertainties calculated for each of the two fractions.

Table 6a. Laboratory A. Mean, standard deviation and CV% as determined for the replicates respectively in the cases of the whole sample and combining data from dust fraction and the fibrous fraction (see text). Calibration has been obtained using averaged response factor (Rf).

Whole sample			
2θ	Average	Std. Deviation	CV%
27,46°	9.62%	±1,07%	±11.1
41,29°	11.12%	±1.54%	±13.8
54,36°	9.63%	±0.99%	±10.2

Table 6b. Laboratory A. Mean, standard deviation and CV% as determined for the replicates respectively in the cases of the whole sample and combining data from dust fraction and the fibrous fraction (see text). Calibration has been obtained using pure standard (100% nominal concentration) single point.

Whole sample			
2θ	Average	Std. Deviation	CV%
27,46°	19.59%	±2.18%	±11.1
41,29°	24.03%	±3.31%	±13.8
54,36°	18.77%	±1.92%	±10.2

In this case the repeatability uncertainty for the entire sample is calculated by combining the repeatability uncertainties of the two individual fractions, using the following formula [15-19]

$uc = \sqrt{[(0.81\ ua)2 + (0.19\ ub)2]}$

where, "a", "b" and "c" represent the average Rutile concentration values for the two dusty (81% by weight) and fibrous (19% by weight) fractions and ("c") the weighted average on the two fractions; where "ua", ub" denote the repeatability uncertainties for the two dusty and fibrous fractions and "uc" indicates the repeatability uncertainty calculated for the weighted average "c".

c±uc = (a±ua)x0.81 + (b±ub)x0.19,

where: c = a*0.81+b*0.19 (weighted average)

and: $uc = \sqrt{[(0.81ua)2 + (0.19\ ub)2]}$ [15-19]

The average results (Rutile concentration) obtained through calibration with a 95% pure standard show much higher values than those obtained through the response factors determined with multiple calibration levels. The loss in linearity for the diffraction signals at concentration values above 50% indicates a poor reliability of the

https://doi.org/10.61577/scpnmia.2025.100003

RESEAPRO JOURNALS

calibration with pure standard and a better choice the use of a multi-level calibration, with the concentration interval centered around the sample concentration (between 10% -20% indicatively, for the present case) if applicable. Furthermore, the substance used for pure standard dilution could influence or interfere on the standard diffraction lines, (similar to how the rate matrix affects them, but potentially in a manner that is either significantly different or negligible).

For XRPD analyses in waste matrices certified reference samples or proficiency testing exercises to verify the accuracy are generally unavailable, except for types of waste that are inherently homogeneous or can be effectively homogenized For this purpose, Laboratory A used some alternative confirmation approaches for accuracy like standard addition methods [8], and analysis by XRD in a different laboratory (Laboratory C) or by different techniques (e.g. XRF) in a different laboratory (Laboratory B).

In the case of the present sample with the XRF technique and using the same multi-level calibration standards to determine the Rf factors, a value equal to 19-20% as titanium dioxide TiO_2 was obtained in another laboratory (Lab B) for the overall waste sample. In Figure 6 the calibration graph for the XRF analyses is reported. It was performed with the same solid solutions used in Laboratory A for the XRD calibration and supplied to Laboratory B. Table 7 presents data for the two fractions of the sample -the powdery and fibrous fractions- as well as data for the overall sample.

Table 7. Laboratory B. XRF control measures for accuracy confirmation of the XRPD data. (1) The mean is exclusively calculated for the data on fibrous fraction. (2) result calculated considering the 81% weight contribution of non-fibrous fraction and the 19% weight contribution of fibrous fraction.

Measure	Non-fibrous fr.	Fibrous fr.	Means[1]	Whole Sample[2]
1	23.4%	-	23.4%	**19.9%**
2-a	-	4.5%	5.3%	
2-b	-	5.4%		
2-c	-	6.0%		

For the fibrous fraction, three replicate measurements were conducted due to the material's greater heterogeneity, whereas only a single measurement was performed on the powdery fraction. Unexpectedly, the value obtained seems more in agreement with the XRPD series obtained using the calibration approach with the pure standard (100% nominal pure Rutile). However, the first XRF measurements do not agree with first XRD results suggesting evidence of bias potentially caused by a loss of linearity in the XRPD calibrations. Additionally, varying responses for Titanium by XRF, depending on the matrix type, cannot be entirely ruled out.

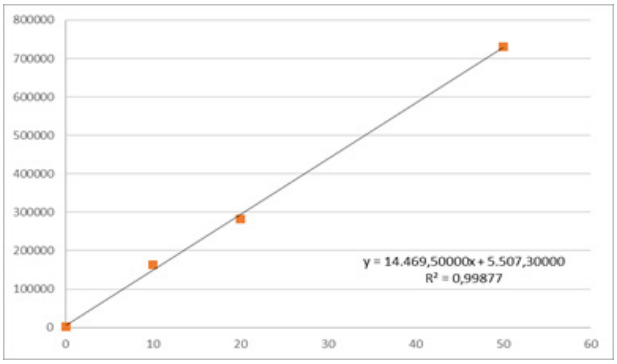

Figure 6. Laboratory B. XRF calibration graph: signal area (arbitrary units) versus TiO_2 nominal concentration (% units). Range from 10% TiO_2 to 50%.

To obtain further experimental evidence, the standard addition method was used with the XRPD technique both at our laboratory (Lab A) and at a second laboratory (Lab C). The results were compared with those obtained with the XRF technique (Lab B), using the standard addition technique. Given the complexity of the sample, consisting of a fibrous fraction and a dusty fraction, and the inherent difficulty of homogenizing these two types of fractions becomes challenging to incorporate a powder (i.e. pure standard) into a fibrous matrix to achieve a homogeneous product. Due to these difficulties the experiments with standard additions were carried out only on the dusty fraction of the sample and therefore they were compared only with the data in Tables 3a and 3b (XRPD) and the data relating to the dusty fraction in Tables 5a, 5b (XRPD) and Table 7 (XRF).

Figure 7 shows the standard additions performed at Laboratory A on the dusty fraction of the sample, for the diffraction lines at 2θ = 27.46°, 36.10°, 41.29° and 54.36°. In this case the waste matrix does not interfere with the signal at 2 = 36.10° and therefore this diffraction line was also used.

The graphs corresponding the signals at 2 = 27.46° and 36.10° indicate that the point corresponding to the addition of 20% (nominal concentration) of TiO2 begins to deviate from linearity. This results in a calibration curve with a reduced coefficient of determination (R^2), making it unsuitable for inclusion in the standard addition analysis. The measurement of the "zero addition" point, i.e. corresponding to the waste sample as it is, was replicated three times.

Laboratory C proceeded with the standard addition through three independent experiments of standard additions, on the dusty fraction of the sample provided by Laboratory A. Figure 8 illustrates the quantification of Rutile on the waste sample as determined by adding the signals at 2 = 36.03°-36.06° and 2 = 36.12°-36.15° (the instrument in this case allows the partial resolution of two very close signals, partly overlapping).

In this case the loss of linearity becomes evident at the addition point at the concentration level of 15% (nominal) TiO2 (Figure 8, left) with a value lower than 0.9 of the coefficient of variation R2. Consequently, this point, along with the 20% nominal TiO2 addition point was excluded from the

https://doi.org/10.61577/scpnmia.2025.100003

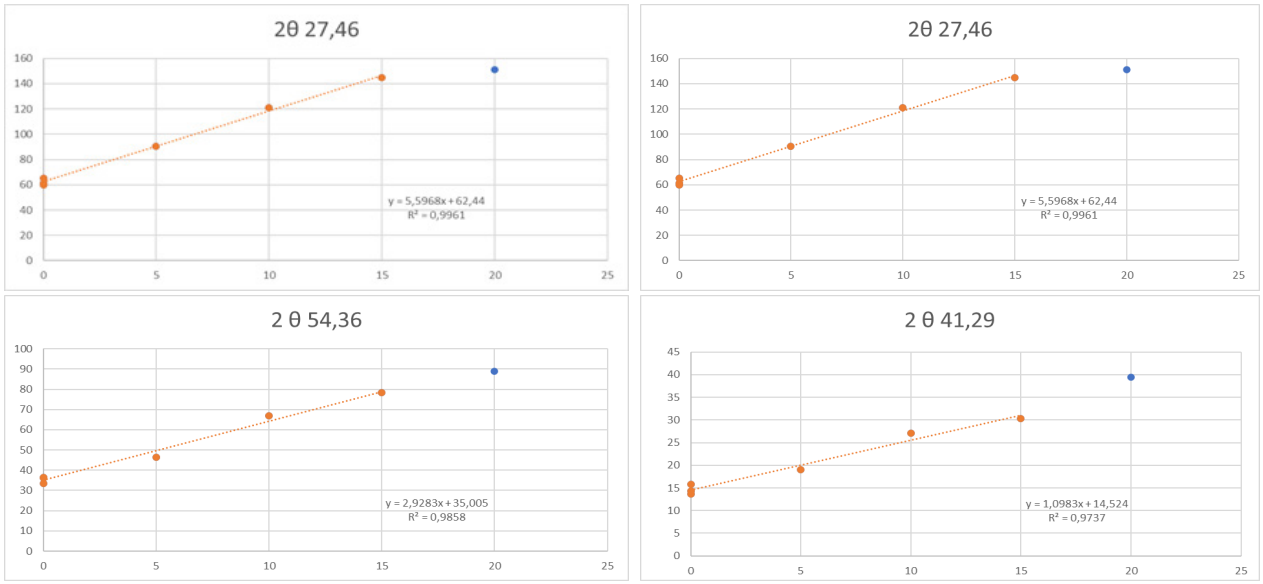

Figure 7. Laboratory A. XRPD standard addition calibration graph: signal area (arbitrary units) versus TiO_2 nominal concentration (% units). Range from 10% to 20% TiO_2 addition.

analysis (Figure 8, right), By doing so, a more acceptable R^2 value, exceeding 0.95 was achieved.

Figure 9 shows the quantitation by standard addition carried out at Laboratory B, with the XRF technique. In this analysis, a loss of linearity was observed at higher addition levels. However, considering the addition level up to 15% (nominal) addition of TiO_2, the obtainable linearity was acceptable and better (R2 = 0.98) than the one including the addition point at the nominal TiO_2 concentration level of 20% (R2 = 0.95).

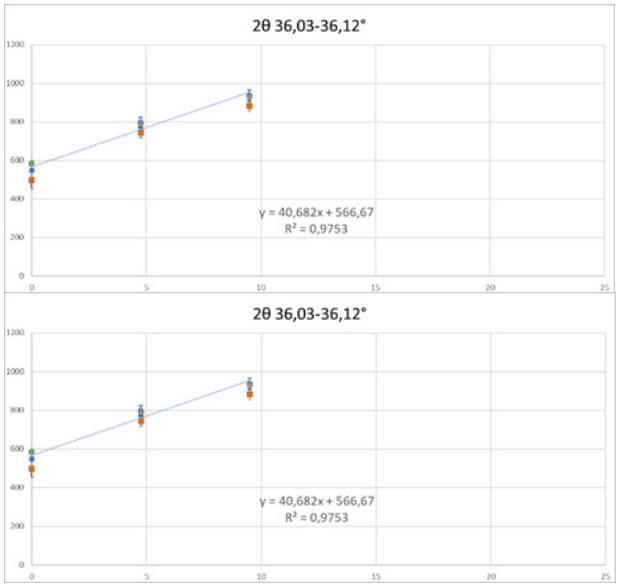

Figure 8. Laboratory C. XRPD standard addition calibration graph: signal area (arbitrary units) versus TiO_2 nominal concentration (% units). Range from 10% to 20% TiO_2 addition. Right: addition points considered: 0%, 5%, 10% and 15%. Left: addition points considered: 0%, 5% and 10%.

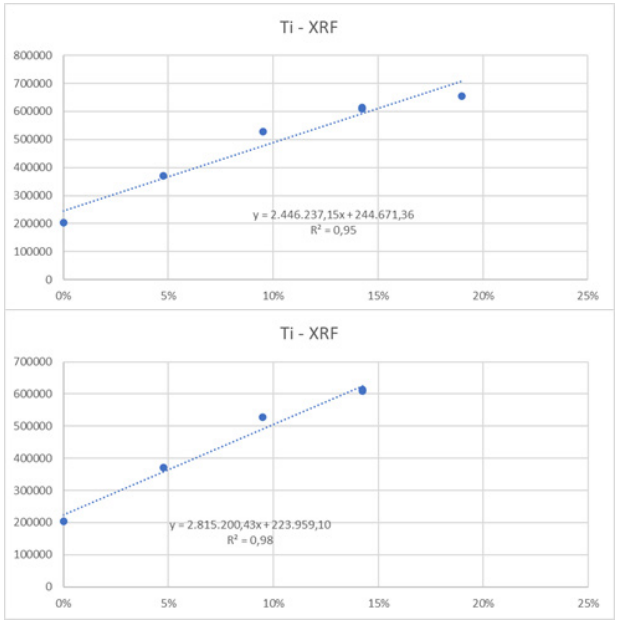

Figure 9. Laboratory B. XRF standard addition calibration graph: signal area (arbitrary units) versus TiO_2 nominal concentration (% units). Range from 10% to 20% TiO_2 addition. Right: addition points considered: 0%, 5%, 10%, 15% and 20%. Left: addition points considered: 0%, 5%, 10% and 15%.

Table 8 lists the results of the standard addition approaches of the three laboratories A, B and C compared. The data from Laboratory B seems to be very different from those obtained by means of calibration with dilutions of the pure Rutilus standard in Extrelut (Tab.7 and Fig. 5). This could indicate a significant matrix effect also present in the XRF approach.

However, it must be noted that in the case of Table 8 the values obtained between laboratories A and B are more in

https://doi.org/10.61577/scpnmia.2025.100003

RESEAPRO JOURNALS

agreement, especially if we take into consideration the data of Laboratory C with its independent determination in XRPD, with the addition method standard. Better reliability of the accuracy data obtained from the comparisons in Table 8 could be achieved associating the results with a measurement uncertainty, which can be determined for Laboratory A.

Table 8. Standard addition experiments for accuracy in Laboratories A, B and C: %TiO_2 content results obtained on the dust fraction of the waste sample.

Standard addition experiment	%TiO_2 content on dust fraction		Technique
Lab A - 2θ 27.46°	11.5%	Mean value: 12.1%	XRD
Lab A - 2θ 36.01°	12.7%		
Lab A - 2θ 41.29°	13.9%		
Lab A - 2θ 54.36°	11.5%		
Lab C - 2θ 36.12°	10.5%		XRD
Lab B - XRF	7.9%		XRF

For Laboratory A, the measurement uncertainty estimate can be done with a metrological approach considering the contribution of the repeatability uncertainty (Tables 6a-6b), the calibration uncertainty (Table 2) and the contributions to the uncertainty due to the errors and inaccuracies of weighings in the preparation of standards. Since proficiency testing exercises or certified waste matrices are not available, studies with holistic approaches to the study of uncertainty are not possible in the present case. In the metrological approach, Within the metrological approach, the uncertainty contribution related to the recovery factor is not considered. This is because the sample preparation does not involve extraction or digestion steps, eliminating the need for further correction of the results for this factor.

The contribution to calibration uncertainty is also simplified by considering that the calibration response factor must be within a fixed acceptability range i.e. ±30% (all the CV% values of the Rf, estimated on considered lines at various diffraction angles listed in Table 2, fall within this criterion). About the errors related to the preparation of the standards we decided to consider another fixed "a priori" precautionary interval equal to ±5% (in any case, the 95% purity of the Rutilus standard was considered in the calculations). The error introduced by the scale of ±0.0001 g on applied to the minimum standard weight carried out for the calibrations (0.2g on a 2 g sample) is equal to ±0.05%. This error is negligible compared to the precautionary interval adopted. Table 9 lists the considered contributions to the combined uncertainty: the "fixed" contributions (type B) with an assumed rectangular distribution identified for the calibration uncertainty and the reference standard equal to ±0.3 and ±0.05 respectively (in relative terms) divided by the √3 term they become ±0.173 and ±0.0289. The type A contributions relating to the repeatability uncertainty are those of Table 6a and 6b.

Table 9. Uncertainty assessment -simplified metrology approach - for the whole sample and for the dust fraction. (1) contributions set as fixed intervals of acceptability; (2) weighed and approximated mean of 6 replicates for dust fraction and 14 replicates for fibrous fraction (14x0.19) + (6x0.81) ≈ 8.

Uncertainty contribution	Type	Whole sample	Dust fraction
Repeatability relative uncertainty	A	±0.138	±0.144
Replicate number (repeatability)		8[2]	6
Calibration relative uncertainty	B[1]	±0.173	±0.173
Standard preparation relative uncertainty	B[1]	±0.0289	±0.0289
Combined relative uncertainty		±0.223	±0.227
Degrees of freedom, effective		45	31
Coverage factor, k		2.02	2.04
Expanded relative uncertainty		±0.45	±0.46

For a better comparison of the experiments in Table 8, Table 9 also reports the uncertainty estimated on the dusty fraction alone. The high degrees of freedom obtained result from assuming fixed contributions "a priori" for calibration uncertainty and related to preparation of the standards. In the Welch-Satterthwaite equation used to calculate the combined degrees of freedom, the relative contributions from these sources, treated as having an infinite number of degrees of freedom, effectively approach zero. As a result, the repeatability uncertainty contribution becomes the predominant factor.

The relative repeatability uncertainty value for the whole sample is derived by combining the absolute uncertainties of the two fractions, weighted their respective percentages, dividing by the combination of the average %Rutile values found on the two fractions, weighted by the respective weight percentages. The relative repeatability uncertainty for the whole sample (0.138) was slightly lower than the one calculated for the dusty fraction alone (0.144). These differences have a negligible impact on the combined uncertainty as does the contribution related to the standard preparation.

In both cases of Table 9 the expanded uncertainty estimated for the present study is within a value of ±50%. Reconsidering the results of the quantitation experiments, using the standard addition method, associated with the estimated uncertainty, the Rutile content value estimated in Table 8 by Lab A and equal to 12.1% is not significantly different from the values estimated by Labs B and C, indicating an acceptable accuracy for the standard additions approaches. This indicates acceptable accuracy for the approach with external standard calibration (Rf) on multiple levels (see average values for the non-fibrous fraction of Table 5-a). While the single point method with pure standard can be prone to significant errors in case of deviations from the linearity of the analytical response.

https://doi.org/10.61577/scpnmia.2025.100003

Conclusion

A case study was illustrated for the uncertainty estimation approach to a particularly complex waste matrix. Analytical methods that perform determinations at levels of g/100g can usually exhibit expanded uncertainties between ±5 and ±20% depending on the type of determination. The high estimated expanded uncertainty value (±50%) is also due to several difficulties (non-homogeneity, matrix effects) encountered in waste matrices.

The study highlighted that operating with an external standard can be acceptable but subject to some problems: calibrating with a single point pure standard allows for greater speed but can give significant bias if the linearity of the response is not respected throughout the range 0-100%. On the other hand, creating a calibration curve or determining the Rf response factor on multiple levels, these include the need to identify a suitable powdered dilution substance that does not produce interfering diffraction lines on the analyte signals, does not distort the baseline, and does not introduce matrix effects that could influence the analyte response.

The standard addition method appears to be the best approach to obtain acceptable results. Adding the pure standard directly to the sample matrix allows for the direct consideration of any effects associated with the waste matrix. It also eliminates the need to dilute the standard by dispersion and mixing with other powdered solids. This approach becomes important in the case of public waste control where in each analysis request you may have to deal with different analytes and different matrices. Given the challenge of obtaining sufficient quantities of pure standard compounds or materials to cover all possible analytes detectable in samples, the use of an internal standard with the Relative Intensity Ratio (RIR) method could be highly advantageous. However, for waste matrices, it is crucial to assess whether matrix effects could alter the intensity ratio between the diffraction lines of the internal standard and those of the target analyte, compared to the tabulated values in the RIR approach. This evaluation is essential to ensure the accuracy and reliability of the method in complex matrices.

Acknowledgements

The technical support in XRPD measurements of Stefania Marmai and Massimiliano Santacroce (Laboratory A) is herewith acknowledged.

Disclosure statement

No funds, grants or other supports were received for this work. The authors declare no potential conflict of interest or involvement in any organization or entity with any financial interest or non-financial interest in the subject matter or materials discussed in this manuscript.

References

1. Waste Framework Directive (2008/98/EC). European Environment Agency. 2008. https://www.eea.europa.eu/ds_resolveuid/e6a52aa01a8db261a66c055b1ec4b787
2. Waste Framework Directive (2008/98/EC). PROPERTIES OF WASTE WHICH RENDER IT HAZARDOUS. European Environment Agency. 2008. https://www.eea.europa.eu/ds_resolveuid/e6a52aa01a8db261a66c055b1ec4b787
3. COMMISSION REGULATION (EU) No 1357/2014. European Parliament and of the Council on waste and repealing certain Directives. 2014. http://data.europa.eu/eli/reg/2014/1357/oj
4. COUNCIL REGULATION (EU) 2017/997. European Parliament and of the Council as regards the hazardous property HP 14 'Ecotoxic'. 2017. http://data.europa.eu/eli/reg/2017/997/oj
5. Non-destructive testing - X-ray diffraction from polycrystalline and amorphous materials - Part 2: Procedures. BRITISH STANDARD. 2003.
6. U.S. EPA. "Method 8260D (SW-846): Volatile Organic Compounds by Gas Chromatography/Mass Spectrometry (GC/MS),". 2006. Washington, DC. https://www.epa.gov/esam/epa-method-8260d-sw-846-volatile-organic-compounds-gas-chromatography-mass-spectrometry-gcms
7. U.S. EPA. "Method 8270E (SW-846): Semivolatile Organic Compounds by Gas Chromatography/ Mass Spectrometry (GC/MS),". 2014. Washington, DC. https://www.epa.gov/esam/epa-method-8270e-sw-846-semivolatile-organic-compounds-gas-chromatographymass-spectrometry-gc
8. Non-destructive testing - X-ray diffraction from polycrystalline and amorphous material - Part 1: General principles. iTeh STANDARD. 2003. https://standards.iteh.ai/catalog/standards/sist/80e37355-dce7-4ee9-92db5357ff7830b2/sist-en-13925-1-2004
9. Siemens Kristalloflex D5000: Mineral & Master libraries databases. EVA 2 SocaFile library and AboutBox library. 2002.
10. Lafuente B, Downs RT, Yang H, Stone N, Armbruster T, Danisi RM. The power of databases: the RRUFF project. Highlights in mineralogical crystallography. 2015;1:25. Berlin, München, Boston: De Gruyter. https://doi.org/10.1515/9783110417104-003
11. Marmai S, Rinaldi L, Calvisi F, Volante M. Interference from Titanium Carbide and Graphite in the determination of Total Organic Carbon (TOC) in waste. Case studies and in-depth studies by X-ray diffraction. Bull Environ Stud. 2016;3:37-44.
12. Hillier S. Accurate quantitative analysis of clay and other minerals in sandstones by XRD: comparison of a Rietveld and a reference intensity ratio (RIR) method and the importance of sample preparation. "Clay Miner. 2000;35(1):291-302. https://doi.org/10.1180/000985500546666
13. Hillier S. Quantitative analysis of clay and other minerals in sandstones by X-ray powder diffraction (XRPD). Clay mineral cements in sandstones. 1999:213-251. https://doi.org/10.1002/9781444304336.ch11
14. Quantitative Analysis - Reference Intensity Ratio. International Centre for Diffraction Data. Accessed on 28 May, 2025. https://www.icdd.com/assets/tutorials/Quantitative-Analysis-RIR.pdf
15. PROPAGAZIONE DELLE INCERTEZZE. UNCERTAINTY PROPAGATION. University of Ferrara. Accessed on 28 May, 2025. https://www.unife.it/ing/meccanica/insegnamenti/fisica_generale_I/formulario3.pdf
16. Palmer M. Propagation of Uncertainty through Mathematical Operations. Massachusetts Institute of Technology. http://web.mit.edu/fluids-modules/www/exper_techniques/2.Propagation_of_Uncertaint.pdf
17. Fantner G. A brief introduction to error analysis and propagation. 2013. https://www.epfl.ch/labs/lben/wp-content/uploads/2018/07/Error-Propagation_2013.pdf
18. Rouaud M. Probability, Statistics and estimation: propagation of uncertainties in experimental measurement. Mountain View, CA: Creative Commons. 2013:52-57.
19. Jcgm JC. Evaluation of measurement data—Guide to the expression of uncertainty in measurement. Int Organ Stand. Geneva ISBN. 2008;50:134.

https://doi.org/10.61577/scpnmia.2025.100003